3D Rotation Invariant Local Binary Patterns

J. Fehr and H. Burkhardt

Chair of Pattern Recognition and Image Processing
University of Freiburg, Germany
fehr@informatik.uni-freiburg.de

Abstract

We present a novel method for the fast computation of rotation invariant "local binary patterns" (LBP) on 3D volume data.
Unlike a previous publication on 3D LBP, this new approach is not limited to "uniform patterns", providing a real 3D extension of the standard and rotation invariant LBP. We evaluate our methods in the context of 3D texture analysis of biological data.

1 Introduction

"Local Binary Patterns" (LBP) [7] have been established as a standard feature based method for 2D image analysis. LBP have been successfully applied to a wide range of different applications from texture analysis [7] to face recognition [8]. Various extensions to the basic LBP algorithms were published in recent years, including rotation invariant and computationally efficient "uniform binary patterns" (fuLBP) - a comprehensive overview can be found in [7].

In this paper, we extend the original LBP from 2D images to 3D volume data. We also generalize the rotation invariant LBP, implementing full rotation invariance in 3D.

Related Work. So far, standard LBP have only been applied to 2D images and 2D time series. There are several recent publications on "volume local binary patterns" (vLBP)[10][9][11], but confusingly these methods deal with dynamic texture analysis on 2D time series and not on full 3D volumetric data. Respectively, vLBP only provide rotation invariance towards rotations around the z-axis.

To the best of our knowledge, there has been only one publication on full 3D LBP: previously we introduced a 3D method for the approximate computation of "uniform LBP" (uLBP) in [3]. This first approach

has several drawbacks: Since the number of possible "uniform patterns" is drastically increasing in the 3D case, we had to generate template like, data dependent uLBP. Also, the approximation method does not provide complete gray-scale invariance. With our new method, we are able to cope with these problems.

LBP in 2D. LBP encode the gray-scale invariant pattern of N neighboring pixels with gray values $x_i, i \in \{0 \dots N-1\}$. The neighbors are given as equidistant points on a circle with radius r around a center pixel with gray value c.

$$\mathrm{LBP}_N^r := \sum_{i=0}^{N} \mathrm{sig}(x_i - c) \cdot 2^i \qquad (1)$$

$$\text{with } \mathrm{sig}(x) := \begin{cases} 1 & \text{for } x > 0 \\ 0 & \text{otherwise} \end{cases}$$

For more details on 2D LBP refer to [7].

Rotation Invariance in 2D can be achieved via normalization:

$$\mathrm{rLBP}_N^r := \min(\mathrm{ROT}(LBP_N^r, n)) \qquad (2)$$
$$\text{with } n = 0 \dots N-1$$

Where $\mathrm{ROT}(LBP_N^r, n)$ is a discrete rotation of the neighbors by n steps. More details on rotation invariant 2D LBP can be found in [7].

2 LBP in 3D

At a first glimpse, the extension of LBPs to 3D seems to be straight forward: Simply pick a center voxel with gray value c, and sample a fixed number of N equidistant points with gray values $x_0 \dots x_{N-1}$ on the respective sphere with radius r. Compute $\mathrm{sig}(x_i - c)$ for all x_i and encode the binary pattern as in the usual LBP algorithm.

This appears to be very simple, but one has to face

several severe problems following this direct approach: first, equidistant sampling on a sphere is a very hard task which is known as *Fejes Toth's* problem. In general, it cannot be solved analytically. Since we need equidistant sampling in order to achieve full rotation invariance, we are limited to the few known point sets where a sampling is known [2] or we have to use rather expensive numerical approximations. Secondly, rotation invariant LBPs require an ordering of the sampled points, which is trivial in 2D - but turns out to be a quite hard problem given three degrees of freedom on a sphere. And last, computational complexity becomes an issue with the vast rising number of sampling points needed on a sphere.

Our approach is based on the pre-computation of so-called **2-patterns**. A 2-pattern P_N^r is the volume representation (3D grid) of a set of N equidistant points on a sphere with radius r. Each of theses points is weighted in an arbitrary but fixed order with the gray values $p_0 := 2^0, \ldots, p_{N-1} = 2^{N-1}$. All other points in the volume are set to zero.

For each LBP computation, we generate a volume representation X^r of the gray values of all points on the neighborhood sphere with radius r. Given a center point with gray value c, we then compute the point-wise threshold of the entire volume grid:

$$T^r : \forall t_i \in T^r, x_i \in X^r : t_i := \mathrm{sig}(x_i - c). \quad (3)$$

The resulting LBP is then computed via the dot-product of the 2-pattern and the threshold:

$$\mathrm{LBP}_N^r := <P_n^r, T^r> \quad (4)$$

Hence, given an equidistant sampling, the computation of 3D LBP is not so difficult - the actual problem is to obtain rotation invariance in 3D.

2.1 Rotation Invariance

In the 2D case, where rotations have only one degree of freedom, invariance can be realized via minimum search over all cyclic shifts of the circular 2-pattern in $O(N)$ (2). Using our fixed 2-pattern on a sphere, we now encounter three degrees of freedom. This makes the 3D case a lot more difficult and computationally expensive.

We engage this problem by revising (2): we can reformulate the problem as the computation of the minimum of the full correlation ($\star$) over all angles of the fixed 2-pattern P_r^N with T^r:

$$\mathrm{rLBP}_N^r := \min(P_N^r \star T^r) \quad (5)$$

In the next section, we will show how this correlation can be computed efficiently in the frequency domain.

3 Fast Implementation

3.1 Mathematical Foundations

Let us start with a very brief introduction of the basic mathematical tools and conventions we need to construct a fast correlation on a sphere. Please refer to [5] and [1] for more detailed background on the methods used.

Spherical Harmonics. Spherical Harmonics (SH) [5] form an orthonormal base on the 2-sphere. Analogical to the Fourier Transform, any given real valued signal f on a sphere with its parameterization over the angles Θ, Φ (latitude and longitude on the sphere) can be represented by an expansion in its harmonic coefficients:

$$f(\Theta, \Phi) = \sum_{l=0}^{\infty} \sum_{m=-l}^{m=l} \hat{f}_{lm} Y_m^l(\Theta, \Phi) \quad (6)$$

where l denotes the band of expansion, m the order for the l-th band and $\hat{f}_{lm}$ the harmonic coefficients. The harmonic base functions $Y_m^l(\Theta, \Phi)$ are computed as follows:

$$Y_m^l(\Theta, \Phi) = \sqrt{\frac{2l+1}{4\pi} \frac{(l-m)!}{(l+m)!}} \cdot P_m^l(\cos \Theta) e^{im\Phi}, \quad (7)$$

where P_m^l is the associated Legendre polynomial.

The harmonic expansion of a signal f will be denoted by $\hat{f}$ with corresponding coefficients $\hat{f}_{lm}$. In our case, where we are only considering signals on a discrete grid in $\mathbb{R}^3$, the $\hat{f}_{lm}$ can be computed via point-wise multiplication ($\cdot$) of the 3D data grid with pre-computed discrete approximations of the harmonic base functions of fixed radii:

$$\hat{f}_{lm} = \sum_{\mathbb{R}^3} \overline{Y_m^l} \cdot f \quad (8)$$

Rotations in SH. We use the Euler notation in zyz-convention denoted by the angles φ, θ, ψ with $\varphi, \psi \in [0, 2\pi[$ and $\theta \in [0, \pi[$ to parameterize the rotations $R \in SO(3)$ (short hand for $R(\varphi, \theta, \psi) \in SO(3)$).
Rotations $R(\varphi, \theta, \psi) \cdot f$ in the Euclidean space find their equivalent representation in the harmonic domain in terms of the so called Wigner D-Matrices, which form an irreducible representation of the rotation group $SO(3)$. For each band l, $D^l(\varphi, \theta, \psi)$ (or short handed $D^l(R)$) defines a band-wise rotation in the SH coefficients. Hence, a rotation in the Euclidean space can be estimated in the harmonic domain (with a maximum expansion b) by

$$R \cdot f \approx \sum_{l=0}^{b} \sum_{m=-l}^{l} \sum_{n=-l}^{l} D_{mn}^l(R) \hat{f}_{lm} Y_m^l \quad (9)$$

3.2 Fast Correlation in SH

We are following the fast correlation method which is inspired by [6]. The full correlation function c_{orr} : $SO(3) \to \mathbb{R}$ of two signals f and g under the rotation $R \in SO(3)$ on a 2-sphere is given as:

$$c_{orr}(f, g, R) := \int_{S^2} f \cdot (R \cdot g) \quad d\phi d\theta d\psi \qquad (10)$$

Using the DFT Convolution Theorem and substituting f and g with their SH expansions (9, 8) leads to

$$c_{orr}(f, g, R) = \sum_{lmn} \overline{D^l_{mn}(R)} \hat{f}_{lm} \overline{\hat{g}_{ln}} \qquad (11)$$

The actual "trick" to obtain the fast correlation is now to factorize the original rotation $R(\varphi, \theta, \psi)$ into $R = R_1 \cdot R_2$, choosing $R_1(\xi, \pi/2, 0)$ and $R_2(\eta, \pi/2, \omega)$ with $\xi = \varphi - \pi/2, \eta = \pi - \theta, \omega = \psi - \pi/2$.

Using the fact that

$$D^l_{mn}(\varphi, \theta, \psi) = e^{-im\varphi} d^l_{mn}(\theta) e^{-in\psi} \qquad (12)$$

where d^l is a real valued so called "Wigner (small) d-matrix" [1], and

$$D^l_{mn}(R_1 \cdot R_2) = \sum_{h=-l}^{l} D^l_{nh}(R_1) D^l_{hm}(R_2) \qquad (13)$$

we can rewrite the rotation as

$$D^l_{mn}(R) = \sum_{h=-l}^{l} d^l_{nh}(\pi/2) d^l_{hm}(\pi/2) e^{-i(n\xi + h\eta + m\omega)} \qquad (14)$$

Substituting (14) into (11) provides the final formulation of the correlation function regarding the new angles ξ, η and ω:

$$c_{orr}(f, g, \xi, \eta, \omega) = \sum_{lmhn} d^l_{mh}(\pi/2) d^l_{hn}(\pi/2) \cdot \hat{f}_{lm} \overline{\hat{g}_{ln}} e^{-i(n\xi + h\eta + m\omega)} \qquad (15)$$

where l is running from 0 to the maximum band of expansion, and m, h, n from $-l, \ldots, l$. The direct evaluation of this correlation function is of course not possible - but it is rather straight forward to obtain the Fourier transform of (15), hence eliminating the missing angle parameters:

$$\hat{c}_{orr}(f, g, m, h, n) = \sum_{l} d^l_{mh}(\pi/2) d^l_{hn}(\pi/2) \cdot \hat{f}_{lm} \overline{\hat{g}_{ln}} \qquad (16)$$

Finally, the full correlation $(f \star g)$ over all angles (ξ, η, ω) can be retrieved via inverse FFT of the entire grid $\hat{C}_{orr}$ of all possible $\hat{c}_{orr}(m, h, n)$

$$f \star g = FFT^{-1}(\hat{C}_{orr}), \qquad (17)$$

revealing the correlation values on a sparse grid in a three dimensional (ξ, η, ω)-space. The minimum correlation $\min(f \star g)$ is found by searching the grid which has a size of $(2b + 1)^3$, where b is the maximum band. Hence, correlation accuracy and computational complexity are directly linked to the maximum spherical harmonic expansion. Since the grid sizes are still considerably small for any likely b, the full correlation can be computed in a few milliseconds on a standard PC.

3.3 Final Algorithm

Given our fast correlation, we compute the rLBP in three steps: first, compute the 2-pattern P^r_N and T^r using known equidistant samplings [2] with 24 to 124 samples. Then expand both in spherical harmonics and obtain the coefficients $\hat{P}^r_N$ and $\hat{T}^r$ and finally compute the rLBP via the minimum of the fast correlation of $\hat{P}^r_N$ and $\hat{T}^r$ as stated in (5).

3.4 Further Speedup

The actual bottleneck of our approach is the complexity of the computation of T^r which is increasing with the number of sampling points. For full gray-scale invariance we have to compute T^r correctly, but there is an elegant way to approximate $\hat{T}^r$ while preserving a gray-scale robustness: we compute $\hat{X}^r$ and subtract c in the frequency domain, which only affects the 0th coefficient $\hat{T}^r_0$:

$$\hat{T}^r_0 \approx \hat{X}^r_0 - c \cdot b, \qquad \hat{T}^r_i \approx \hat{X}^r_i \qquad (18)$$

Hence, we no longer have a binary but continuous weighting of the n-pattern. We will refer to this approximation as aLBP.

4 Experiments

We evaluated the texture analysis performance of the rLBP and aLBP on 3D volumetric biological data and compared the results to the fuLBP methods presented in [3] and a Haar-Integration approach in[4]. A database containing 229 3D volume datasets of 3 different classes of cell-nuclei was given. The cells were recorded in tissue via confocal laser microscopy using two different anti-body markers, YoPro and Cy3,
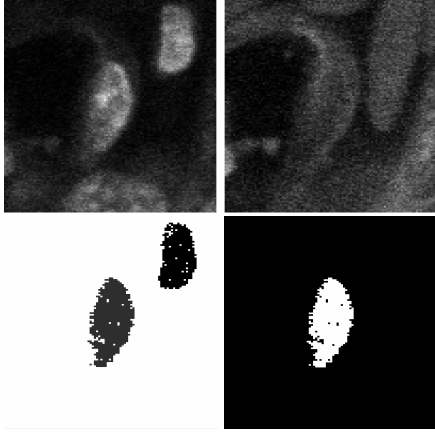
Figure 1. Sample database entry, xy-slices of 3D volumetric data. From left to right: YoPro marker, Cy3 marker, ground truth labeling of the cell nuclei, binary mask for the database entry.

type	result in [4]	fuLBP[3]	rLBP	aLBP
A	93,3%	88,7%	91,3%	90,5%
B	84,6%	75,8%	79,8%	78,2%
C	79,8%	74,2%	75,1%	74,8%
D	94,1%	90,9%	93,4%	91,0%

Table 1. Results of the nuclei classification comparing the Haar-Intergral based features from [4] and fuLBPs with our new approach. The celltypes are A:Erythrocyte, B:Endothelial cell, C: Fibroblast and D:Background.

which were recorded in separate channels. For this experiment, we used only the YoPro channel. A sample database entry is shown in Fig. 1, please refer to [4] for further details on the database.

We used 12 different features of varying radii, number of samples and expansion bands. After feature extraction, we performed a voxel-wise classification via support-vector machine (SVM) following the algorithms in [4]. Results are shown in table 1.

5 Conclusions

We presented a novel method for the computation of rotation invariant 3D LBP for 3D texture analysis on volume data. Our new approach rLBP clearly outperforms the previous fuLBP, and even the approximative aLBP

perform slightly better. However, the main improvement of the general rLBP is the easy handling compared to the fuLBP where one has to perform an elaborate precomputation of the uniform patterns. In terms of computational complexity, the cost of the rLBP depends on the number of samples and can become quite expensive - a tradeoff between resolution and costs. aLBP provide an efficient alternative, if gray scale invariance is not crucial. All LBP methods were outperformed by the Haar-Intergral based features from [4]. The reason for this may be that LPB have a larger spacial resolution, but a weaker gray scale resolution than Haar-features - which might be not favorable for the given task.

References

[1] D. Brink and G. Satchler. *Angular Momentum, Second Edition*. Clarendon Press, Oxford, 1968.

[2] H. Cundy and A. Rollett. *Mathematical Models*. Oxford Univ. Press, 2nd ed., 1961.

[3] J. Fehr. Rotational invariant uniform local binary patterns for full 3d volume texture analysis. In *Proc. FinSig 2007*, 2007.

[4] J. Fehr, H. Kurz, C. Sauer, and H. Ronneberger, O.and Burkhardt. Identifikation von zellen in intaktem gewebe - selbst-lernende segmentierung und klassifikation von zellkernen in 3d volumendaten mittels voxelweiser grauwertinvarianten. In *Handels H. Ehrhardt J. Editors, Informatik Aktuell, Bildverarbeitung fr die Medizin 2006, Hamburg 19. - 21.3.06*, pages 368–373. Springer-Verlag, 2006.

[5] H. Groemer. *Geometric Applications of Fourier Series and Spherical Harmonics*. Cambridge University Press, 1996.

[6] J. A. Kovacs and W. Wriggers. Fast rotational matching. *Acta Crystallogr*, (58):1282–1286, 2002.

[7] T. Mäenpää and M. Pietikäinen. In C. Chen and P. Wang, editors, *Handbook of Pattern Recognition and Computer Vision*, chapter Texture analysis with local binary patterns., pages 197–216. World Scientific, 2005.

[8] H. Yang and Y. Wang. A lbp-based face recognition method with hamming distance constraint. In *ICIG '07: Proceedings of the Fourth International Conference on Image and Graphics*, pages 645–649, Washington, DC, USA, 2007. IEEE Computer Society.

[9] G. Zhao and M. Pietikäinen. Dynamic texture recognition using volume local binary patterns. In *Proc. ECCV 2006 Workshop on Dynamical Vision*, page 12 pp, Graz, Austria, 2006.

[10] G. Zhao and M. Pietikäinen. Dynamic texture recognition using local binary patterns with an application to facial expressions. *IEEE Transactions on Pattern Analysis and Machine Intelligence*, 29(6, in press.), 2007.

[11] G. Zhao and M. Pietikäinen. Improving rotation invariance of the volume local binary pattern operator. In *Proc. IAPR Conference on Machine Vision Applications*, pages 327–330, Tokyo, Japan, 2007.